IEEE Access
Multidisciplinary | Rapid Review | Open Access Journal

Received January 5, 2020, accepted February 1, 2020, date of publication February 20, 2020, date of current version March 2, 2020.

Digital Object Identifier 10.1109/ACCESS.2020.2975379

Design of Notched-Wideband Bandpass Filters With Reconfigurable Bandwidth Based on Terminated Cross-Shaped Resonators

XIAO-KUN BI[1], XIAO ZHANG[1], (Member, IEEE), SAI-WAI WONG[2], (Senior Member, IEEE), SHAO-HUA GUO[3], AND TAO YUAN[1,4], (Member, IEEE)

[1]Guangdong Provincial Mobile Terminal Microwave and Millimeter-Wave Antenna Engineering Research Center, College of Information Engineering, Shenzhen University, Shenzhen 518060, China
[2]College of Electronics and Information Engineering, Shenzhen University, Shenzhen 518320, China
[3]Institute of Underground Engineering, School of Water Conservancy and Environment, Zhengzhou University, Zhengzhou 450001, China
[4]ATR National Key Laboratory of Defense Technology, College of Electronics and Information Engineering, Shenzhen University, Shenzhen 518060, China

Corresponding author: Xiao Zhang (xiao.zhang@szu.edu.cn)

This work was supported in part by the National Natural Science Foundation of China under Grant 61801298, in part by the Natural Science Foundation of Shenzhen University under Grant 2019118, and in part by the Fundamental Research Program of Shenzhen Science and Technology Innovation Committee, China, under Project JCYJ20180305124721920.

ABSTRACT In this paper, a series of novel reconfigurable-bandwidth notched-wideband bandpass filters (NWB BPFs) with controllable notch bands are proposed. The proposed filters start from a passive filtering structure, which is formed by a terminated cross-shaped resonator (TCSR) with a pair of parallel-coupled lines and two open-ended stubs. Theoretical analysis finds that the filter bandwidth can be independently controlled by the TCSR, while the center frequencies and bandwidth of notch bands are mainly controlled by the rest parts. According to this, a BPF with controllable notch bands can be designed. To achieve the reconfigurable-bandwidth NWB BPFs with controllable notch band, whose bandwidth and center frequency can be maintained unchanged under different work states, two PIN diodes and a varactor are employed. By controlling the work states of PIN diodes, three bandwidth states can be achieved with fixed center frequency. By controlling the applied voltage on the varactor, other NWB BPF with independently tunable lower passband edge can be realized. For verification, three prototypes are designed and measured. The measured results agree well with the theoretical analysis and simulated ones, verifying a simple and effective design approach of reconfigurable-bandwidth NWB BPFs.

INDEX TERMS Notched-wideband bandpass filter (NWB BPF), terminated cross-shaped resonator, PIN diode and varactor, reconfigurable bandwidth, controllable notch bands.

I. INTRODUCTION

Because of the desired properties, i.e., low cost and profile, compact size, and easy integration with other devices, the microstrip filters have been extensively used in the wireless communications systems, such as, 4G, WiFi, and sensing radars. To satisfy different requirements, the microstrip filters with individual characteristics have been designed, including low-pass filters [1], wideband bandpass filters (BPFs) [2]–[4], balanced BPFs [5]–[7], multi-band BPFs [8]–[11], and high-pass filters [12].

In the high data-rate and multi-standard remote-sensing and telecommunication systems, notched-wideband (NWB) BPFs with good filtering responses are urgently needed to eliminate the unexpected in-band interference. Recently, such filters have been designed by different techniques, which can be classified into four main categories: 1) the introduction of additional notch resonators [13] – [15]; 2) asymmetrical coupled fed lines [16], [17]; 3) embedded open stubs [18], [19]; 4) intrinsic zeros of multi-mode resonators (MMRs) [20], [21]. Although all the above filters can own excellent filtering responses and desired notch band simultaneously, they still cannot satisfy the demands of modern multi-standard transceivers, which need NWB BPFs owning different

The associate editor coordinating the review of this manuscript and approving it for publication was Abhishek K. Jha.

reconfigurabilities to reduce the design complexity and system size.

The reconfigurable NWB BPFs have been studied over ten years [22] – [29]. Previous works are mainly focused on the reconfigurable notch band(s) and fixed bandwidth [22] – [27]. For the NWB BPFs with reconfigurable bandwidth, little effort has been devoted, except for some ones in [28], [29], which suffer from many drawbacks including non-electrically reconfigurable, uncontrollable notch bandwidth, and varied center frequencies and bandwidth of notch bands under different work states. Due to the lack of study on the reconfigurable-bandwidth NWB BPFs, the development of telecommunication will be largely restricted. To tackle this, it is very significant to explore different topologies for the design of NWB BPFs with a new reconfigurable-bandwidth property in designing multi-standard advanced transceivers for the practical applications of high-performance circuits and systems.

In this paper, a class of new reconfigurable-bandwidth NWB BPFs with controllable notch band are presented. The proposed design starts from a passive fundamental topology, which is composed of a terminated cross-shaped resonator (TCSR) with some added parts, including two open-ended stubs and a pair of parallel-coupled lines (PCLs). After theoretical analysis, it is found that the filter bandwidth is determined by the characteristic impedances of TCSR, and the notch bandwidth is mainly controlled by the ones of the added parts. Furthermore, the center frequencies of notch bands are totally controlled by the electrical length of open-ended stubs. As such, a NWB BPF with controllable notch bands can be designed. In addition, some reconfigurable-bandwidth NWB BPFs with controllable notch band, whose bandwidth and center frequency are fixed under different work states, can be realized by inserting two PIN diodes and a varactor into TCSR. By controlling the work states of PIN diodes, the lower and upper passband edges can be shifted in same absolute ranges. By controlling the applied voltage on the varactor, the lower passband edge can be independently reconfigurable in continuous manners. Thus, two kinds of reconfigurable NWB BPFs with fixed center frequency and bandwidth of the controllable notch band can be designed, including one with fixed center frequency, and the other one with fixed upper passband edge. To validate this, three prototypes are fabricated and measured. To the best knowledge of authors, such reconfigurable-bandwidth BPFs with controllable notch band, whose center frequency and bandwidth are fixed under different work states, have never been reported before.

This paper is organized as follows. Besides the introduction in Section I, the discussion of the fundamental topology with an emphasis on the transmission poles and zeros is presented with the design of a basic NWB BPF. In Section III, the design of reconfigurable-bandwidth NWB BPFs in discrete and continue manners are presented with the simulated and measured results. Finally, a conclusion is summarized in Section IV.

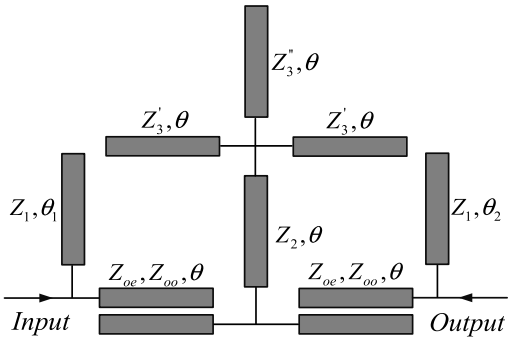

FIGURE 1. Topology of the fundamental NWB BPF (Filter I).

II. BASIC THEORY AND NWB BPF

In Fig. 1, the fundamental topology for the design of a NWB BPF with controllable notch bands is plotted. The fundamental topology is constructed by a TCSR with a pair of PCLs and two open-ended stubs. For the TCSR, its electrical length is $\theta = \pi/2$ at the center frequency f_0, while characteristic impedances are Z_2, Z_3', and Z_3'', respectively. Thus, the input impedance of the TCSR can be written as

$$Z_{in}^{TCSR} = jZ_2 \frac{Z_2 \tan^2\theta - Z_3}{(Z_2 + Z_3)\tan\theta} \tag{1}$$

where

$$Z_3 = \frac{2Z_3'Z_3''}{2Z_3' + Z_3''}. \tag{2}$$

From Eq. (1), we can know that the used TCSR owns one pole f_{p1}^{TCSR} and two zeros $f_{z1}^{TCSR}, f_{z2}^{TCSR}$. For arbitrary Z_2, Z_3', Z_3'', the relationship of $f_{z1}^{TCSR} < f_{TCSR}^{p1} = f_0 < f_{z2}^{TCSR}$ holds. To incorporate the TCSR for a BPF with controllable notch bands, extra poles and zeros should be introduced. Hence, a pair of PCLs with two open-ended stubs are added. For the PCLs, its electrical length is $\theta = \pi/2$ at the center frequency f_0 and characteristic impedances are Z_{oe}, Z_{oo}, respectively. For the open-ended stubs, its electrical length is θ_1 and θ_2, and characteristic impedance is Z_1.

A. TRANSMISSION POLES AND ZEROS

When $\theta_1 = \theta_2 = \theta$, the fundamental topology is symmetrical. Under this condition, its transmission poles (TPs) can be determined by even-odd-mode analysis method. The odd- and even-mode equivalent circuits are shown in Fig. 2 (a) and (b), respectively. For the odd-mode input admittance Y_{ino} in Fig. 2(a), it can be expressed as

$$Y_{ino} = j\frac{1}{Z_1}\tan\theta + \frac{2jA\tan\theta}{A^2 - B^2 - B^2\tan^2\theta} \tag{3}$$

where

$$A = Z_{oe} + Z_{oo}, B = Z_{oe} - Z_{oo}. \tag{4}$$

When Y_{ino} is zero, the odd-mode resonant frequencies can be determined. As such, a pair of odd-mode TPs can be

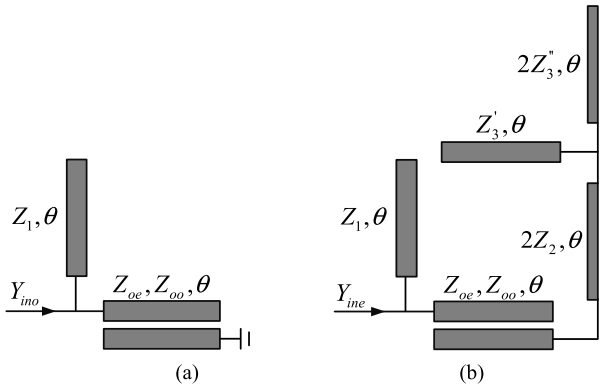

FIGURE 2. (a) Odd- and (b) even-mode equivalent circuits of Filter I.

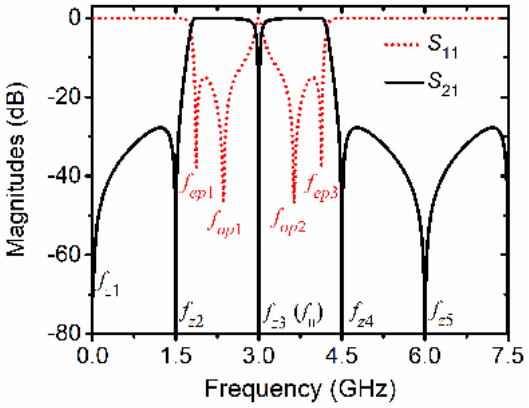

FIGURE 3. The calculated frequency responses of the ideal circuit in Fig. 1 ($Z_1 = 1700\ \Omega$, $Z_2 = 65\ \Omega$, $Z_3 = 65\ \Omega$, $Z_{oe} = 162\ \Omega$, and $Z_{oe} = 58\ \Omega$).

obtained as

$$f_{op1} = \frac{2f_0}{\pi}\arctan\sqrt{\frac{A^2 - B^2 + 2AZ_1}{B^2}} \tag{5a}$$

$$f_{op2} = 2f_0 - \frac{2f_0}{\pi}\arctan\sqrt{\frac{A^2 - B^2 + 2AZ_1}{B^2}} \tag{5b}$$

For the even-mode input admittance Y_{ine} in Fig. 2(b), it can be expressed as

$$Y_{ine} = j\frac{1}{Z_1}\tan\theta + Y_{ine}^R \tag{6}$$

with

$$Y_{ine}^R = \frac{2A\tan\theta + 4jZ_{in}^{TCSR}\tan^2\theta}{2AZ_{in}^{TCSR}\tan\theta - j\left(A^2 - B^2 - B^2\tan^2\theta\right)}. \tag{7}$$

When Y_{ine} is infinite, the even-mode resonant frequencies can be derived. After some algebraic operations, three even-mode TPs can be obtained and expressed as

$$f_{ep1} = f_0 - \frac{2f_0}{\pi}\arctan\sqrt{\frac{\beta}{\alpha}} \tag{8a}$$

$$f_{ep2} = f_0 \tag{8b}$$

$$f_{ep3} = f_0 + \frac{2f_0}{\pi}\arctan\sqrt{\frac{\beta}{\alpha}} \tag{8c}$$

where

$$\alpha = 2AZ_2^2 + (Z_2 + Z_3)B^2 + 4Z_1Z_2^2 \tag{9a}$$

$$\beta = 2(A+2)Z_2Z_3 + \left(A^2 - B^2 + 2AZ_1\right)(Z_2 + Z_3). \tag{9b}$$

For the transmission zeros (TZs), they can be used to achieve notch bands, wide stopbands, and sharp selectivity. Its TZs are determined by rigorous odd-even-mode analysis method and S-parameter theory together. The transmission coefficient can be expressed [30] as

$$S_{21} = \frac{Y_0^2 - Y_{ine}Y_{ino}}{(Y_0 + Y_{ino})(Y_0 + Y_{ine})} \tag{10}$$

where Y_0 is the normalized admittance. Under the condition that $S_{21} = 0$, five TZs can be derived and written as

$$f_{z1} = 0, \quad f_{z3} = f_0, \ f_{z5} = 2\pi \tag{11a}$$

$$f_{z2} = \arctan\sqrt{\frac{Z_3}{Z_2}} \tag{11b}$$

$$f_{z4} = 2\pi - \arctan\sqrt{\frac{Z_3}{Z_2}}. \tag{11c}$$

According to the above theoretical analysis, it is obvious that the fundamental topology owns five TPs and five TZs when the electrical length is uniform. All the TPs/TZs are symmetrical to the center frequency f_0, and the relationship of $f_{z1} < f_{z2} < f_{ep1} < f_{op1} < f_{z3} = f_{ep2} = f_0 < f_{op2} < f_{ep2} < f_{z4} < f_{z5}$ always holds for arbitrary Z_1, Z_2, Z_3, Z_{oe}, Z_{oo}. Considering that the effect of f_{ep2} on filter performance is eliminated by f_{z3} when the electrical length is uniform, the fundamental topology is suitable to design BPFs with a notch band at the center frequency, whose calculated frequency responses are shown in Fig. 3. For the TZs of f_{z1} and f_{z5}, they are used to ensure the wide stopband; for the TZs of f_{z2} and f_{z4}, they are used to sharp the skirt selectivity; for the TZ of f_{z3}, it is used to implement the notch band. For the TPs of f_{ep1}, f_{op1}, f_{op2}, and f_{ep3}, they can be used to ensure the broad and flatness passband. Besides, the filter bandwidth is determined by the TPs of f_{ep1}, f_{ep3} and TZs of f_{z2}, f_{z4} together, while the notch bandwidth is controlled by the TPs of f_{op1} and f_{op2}. To better understand the design mechanism of the fundamental topo-logy, the relationships among the parameters of Z_1, Z_2, Z_3, Z_{oe}, Z_{oo} and TPs/TZs of $f_{z2}, f_{z3}, f_{z4}, f_{op1}, f_{op2}, f_{ep1}, f_{ep2}, f_{ep3}$ are investigated.

The TPs and TZs under investigation respect to different Z_1, Z_2, Z_3, Z_{oe} are shown in Fig. 4. Apparently, the locations of f_{op1} and f_{op2} are mainly controlled by Z_1 and Z_{oe}, while the locations of $f_{ep1}, f_{ep3}, f_{z2}, f_{z4}$ are independently determined by Z_2 and Z_3. With the increase of Z_1 and decrease of Z_{oe}, the TPs of f_{op1} and f_{op2} will move closer to each other. With the increase of Z_2 and decrease of Z_3, the TPs of f_{ep1} and f_{ep3} will move apart, and the same phenomenon is happened to the TZs of f_{z2} and f_{z4} too. Reflected to the filter responses, the filter bandwidth can be independently determined by Z_2 and Z_3, and the notch bandwidth is independently controlled by Z_1

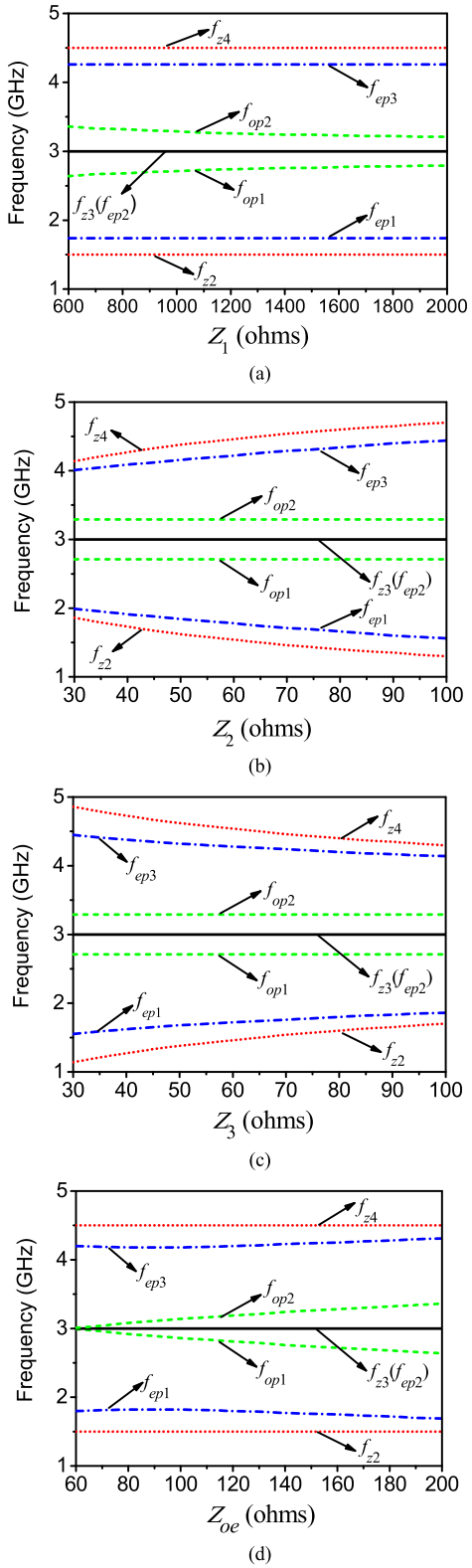

FIGURE 4. The TPs and TZs under investigation respect to different (a) Z_1; (b) Z_2; (c) Z_3; and (d) Z_{oe}. The reference parameters are: $Z_1 = 1700\ \Omega$, $Z_2 = 65\ \Omega$, $Z_3 = 65\ \Omega$, $Z_{oe} = 162\ \Omega$, $Z_{oe} = 58\ \Omega$.

and Z_{oe}. Hence, the filter with wide bandwidth should choose the parameters of Z_2 with large value and Z_3 with small value, while the one with narrow notch bandwidth should choose the

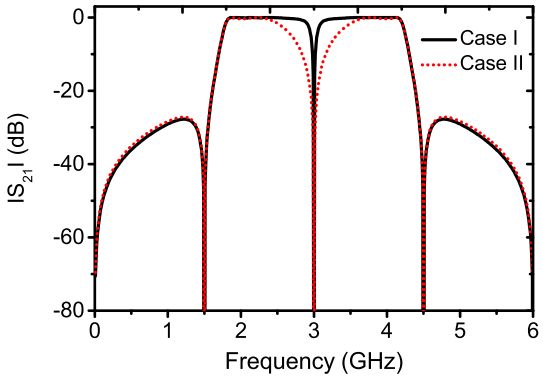

FIGURE 5. The calculated frequency responses of the ideal circuit in Fig. 1 with same filter bandwidth and different notch bandwidth. Case I: $Z_1 = 1700\ \Omega$, $Z_2 = 65\ \Omega$, $Z_3 = 65\ \Omega$, $Z_{oe} = 162\ \Omega$, and $Z_{oe} = 58\ \Omega$. Case II: $Z_1 = 300\ \Omega$, $Z_2 = 65\ \Omega$, $Z_3 = 65\ \Omega$, $Z_{oe} = 170\ \Omega$, and $Z_{oe} = 55.7\ \Omega$.

parameters of Z_1 with large value and Z_{oe} with small value. After slightly adjusting the values of Z_1, Z_2, Z_3, Z_{oe} and Z_{oo} together, the filter with desired responses can be realized.

To vividly demonstrate that the notch bandwidth can be independently controlled, two BPFs with narrow and wide notch bandwidths are illustrated in Fig. 5. Obviously, the notch bandwidth will be changed from narrow to wide by only controlling the parameters of Z_1, Z_{oo}, and Z_{oe}, while the filter bandwidth is maintained unaltered. As such, the notch bandwidth can be independently controlled by Z_1, Z_{oo}, and Z_{oe} together.

B. CONTROLLABLE CENTER FREQUENCIES OF NOTCH BANDS

From Part A, we can know that the notch bandwidth can be independently controlled by the parameters of Z_1, Z_{oo}, and Z_{oe}. To further prevent the wireless communication systems from in-band interfering conveniently and effectively, the center frequencies of notch bands also should be controllable. In this part, the center frequencies of notch bands will be discussed by varying the electrical length of two open-ended stubs.

To vividly demonstrate this, we assume that $\Delta\theta = \theta_1 - \theta = \theta - \theta_2$ at first. Then, the improved topology of Filter I for theoretical analysis is plotted in Fig. 6. When the value of Z_1 is very large, the TPs and TZs under study respect to different $\Delta\theta$ are shown in Fig. 7. Seen from Fig. 7, the TZ of f_{z3} is divided into two ones of f_{z3_L} and f_{z3_U} when $\Delta\theta$ is not equal to zero. With the increase of $\Delta\theta$, the distance between f_{z3_L} and f_{z3_U} will become larger, while the TPs of f_{op1} and f_{op2} move apart. For the rest TPs and TZs, they are fixed. Furthermore, the locations of f_{z3_L} and f_{z3_U} can be determined as

$$f_{z3\_L} = \frac{\theta}{\theta_1} f_0 \tag{12a}$$

$$f_{z3\_U} = \frac{\theta}{\theta_2} f_0. \tag{12b}$$

Considering the filter responses, the proposed topology will own two notch bands when the electrical length θ_1 and

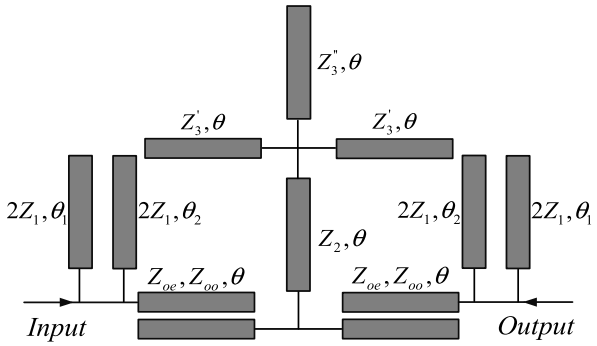

FIGURE 6. Improved topology of Filter I for the theoretical analysis.

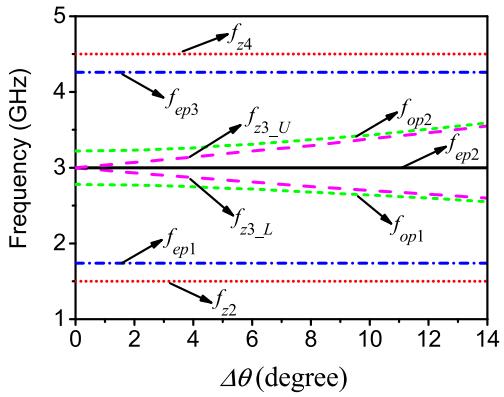

FIGURE 7. TPs and TZs under investigation respect to different $\Delta\theta$. The reference parameters are: $Z_1 = 1700\ \Omega$, $Z_2 = 65\ \Omega$, $Z_3 = 65\ \Omega$, $Z_{oe} = 162\ \Omega$, $Z_{oe} = 58\ \Omega$.

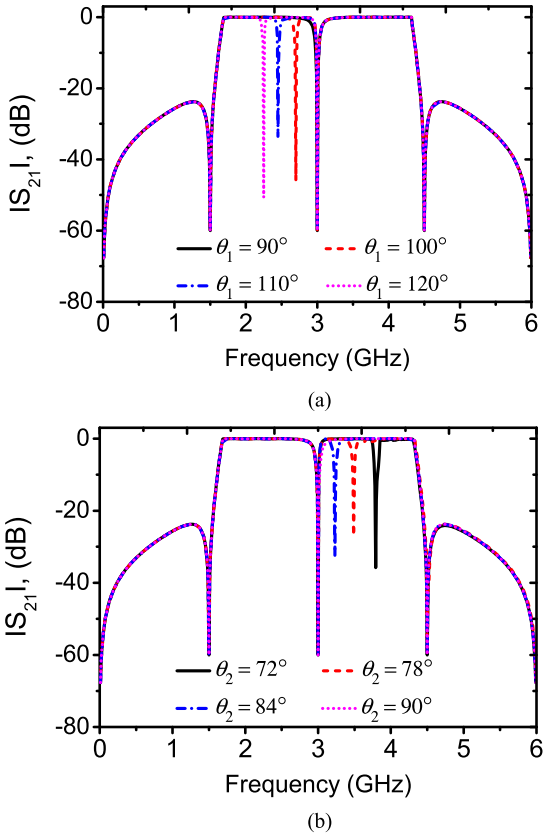

FIGURE 8. The calculated frequency responses of the revised topology in Fig. 6 respect to varied (a) θ_1 ($\theta_2 = 90°$); (b) θ_2 ($\theta_1 = 90°$). The reference parameters are: $Z_1 = 1700\ \Omega$, $Z_2 = 65\ \Omega$, $Z_3 = 65\ \Omega$, $Z_{oe} = 162\ \Omega$, $Z_{oe} = 58\ \Omega$.

θ_2 is not equal. With the increase of θ_1, the notch band of f_{z3_L} will move downwards independently, while the notch band of f_{z3_U} and filter bandwidth are unaltered, as plotted in Fig. 8(a). With the decrease of θ_2, the notch band of f_{z3_U} will move upwards independently, while the notch band of f_{z3_U} and filter bandwidth are kept fixed, as shown in Fig. 8(b). Thus, the center frequencies of the notch bands can be independently controlled with the help of the electrical length θ_1 and θ_2. It is noteworthy that: when the electrical length of θ_1 and θ_2 is too large or small, the notch bands will not be existed in the passband.

C. DESIGN PROCEDURE

On the basis of the above theoretical analysis, a simple and effective design procedure for Filter I can be summarized as:

1) Input the specifications of Filter I, such as, center frequency, filter bandwidth, selectivity, notch bands (including center frequencies and bandwidth).
2) For the filter with wide bandwidth, the parameters of Z_2 with large value and Z_3 with small value should be chosen; for the filter with narrow notch bandwidth, the parameters of Z_1 with large value and Z_{oe} with small value should be selected.
3) The center frequencies of notch bands are decided by the values of θ_1 and θ_2.
4) Slightly adjust the parameters of Z_1, Z_2, Z_3, Z_{oe}, Z_{oo}, θ_1 and θ_2 to obtain the desired performances.

Based on this design procedure, the final parameters of a NWB BPF with 3-dB fractional bandwidth (3-dB FBW) of 82.7% and a narrow notch band at center frequency can be determined as: $Z_1 = 1700\ \Omega$, $Z_2 = 65\ \Omega$, $Z_3 = 65\ \Omega$, $Z_{oe} = 162\ \Omega$, $Z_{oo} = 58\ \Omega$, and $\theta_1 = \theta_2 = \theta = 90°$. The corresponding calculated frequency responses are plotted in Fig. 3. As the employed substrate in this paper is Rogers RO4003C with thickness of 0.813 mm and dielectric constant of 3.38, the layout and final dimensions can be determined with the aid of commercial software. The layout is plotted in Fig. 9. One design skill is used in the layout: to enhance the coupling strength of PCLs and reduce the effect of open-ended stubs on filter responses, some parts of the open-ended stubs are parallel with PCLs. The final dimensions are summarized as (Unit: mm): $l_F = 16.2$, $w_F = 0.3$, $s_F = 0.1$, $l^L_{1\_V} = l^R_{1\_V} = 16.2$, $l^L_{1\_H} = l^R_{1\_H} = 0$, $w_1 = 0.3$, $s_1 = 0.3$, $l_2 = 15.7$, $w_2 = 1.4$, $l'_3 = 16.6$, $w'_3 = 0.1$, $l''_{3\_V} = 4.6$, $l''_{3\_H} = 12.1$, $w''_3 = 0.1$. The overall circuit size is 43.0 mm $\times$33.0 mm (0.62 $\lambda_g \times$ 0.48 λ_g, where λ_g is the guided wavelength in the employed substrate at center frequency).

As predicted, the notch bandwidth can be independently controlled by the parameters of w_1, w_F, s_1, and s_F, which are corresponding to the characteristic impedances of Z_1,

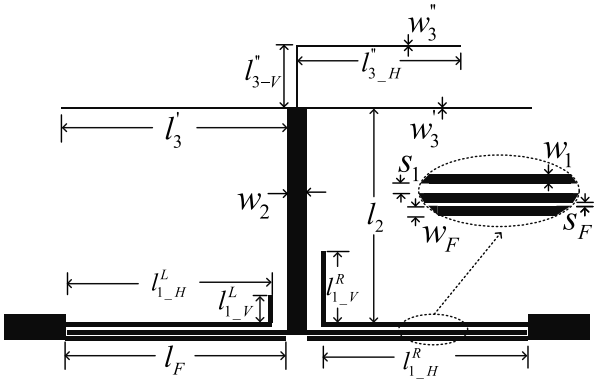

FIGURE 9. The layout of Filter I.

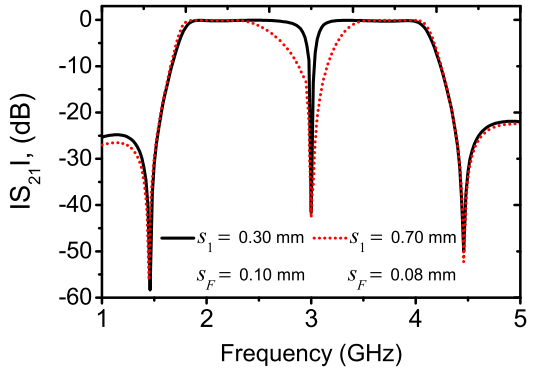

FIGURE 10. The filter responses respect to varied S_1 and S_F. The rest parameters are: l_F = 16.2 mm, w_F = 0.3 mm, w_1 = 0.3 mm, $l_{1\_H}^L = l_{1\_H}^R$ = 16.2*mm*, $l_{1\_V}^L = l_{1\_V}^L$ = 0 mm, l_2 = 15.7 mm, w_2 = 1.4 mm, l_3' = 16.6 mm, w_3' = 0.1 mm, l_{3_V}'' = 4.6 mm, l_{3_H}'' '= 12.1 mm, w_3'' = 0.1 mm.

Z_{oo}, and Z_{oe}. When the parameters of w_1 and w_F are fixed, the notch bandwidth can be varied from narrow to wide by only controlling the parameters of s_1 and s_F, while the filter bandwidth is fixed, as shown in Fig. 10. Hence, the notch bandwidth can be independently controlled.

For the number and center frequencies of the notch bands, they are determined by the physical length of $l_{l\_V}^L$, $l_{l\_V}^H$, $l_{l\_H}^L$ and $l_{l\_H}^R$ together, which are corresponding to the electrical length of θ_1 and θ_2. As predicted, only one notch band is existed in the passband when $l_{l\_V}^L = l_{l\_V}^R$ and $l_{l\_H}^L = l_{l\_H}^R$. In addition, the center frequency of notch band will become smaller with the increase of $l_{l\_V}^L$ ($l_{l\_V}^R$) and $l_{l\_V}^H$ ($l_{l\_H}^R$), as shown in Fig. 11. Under the condition that $l_{l\_V}^L \neq l_{l\_V}^R$ while $l_{l\_H}^L = l_{1\_H}^R$,there are two notch bands existed in the passband. Through increasing $l_{l\_V}^R$ while maintaining $l_{l\_V}^L$, the lower notch band will move downwards while the other one is unaltered, as shown in Fig. 12(a). Meanwhile, there are also two notch bands existed in the passband when $l_{l\_V}^L = l_{l\_V}^R$ while $l_{l\_H}^L \neq l_{l\_H}^R$. As $l_{l\_H}^L$ decreases while $l_{l\_H}^R$ keep unaltered, the upper notch bands will move upwards and the rest one is fixed, which is shown in Fig. 12 (b). According to the above analysis, it is apparent that the center frequencies of notch bands can be independently controlled.

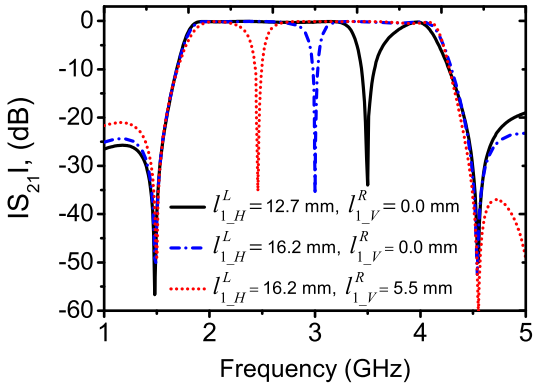

FIGURE 11. The filter responses respect to different $l_{l\_V}^L$ ($l_{1\_V}^R$), $l_{l\_V}^H$ ($l_{1\_H}^R$). The other parameters are: l_F = 16.2 mm, w_F = 0.3 mm, s_F = 0.1 mm, w_1 = 0.3 mm, s_1 = 0.3 mm, l_2 = 15.7 mm, w_2 = 1.4 mm, l_3' = 16.6 mm, w_3' = 0.1 mm, l_{3_V}'' = 4.6 mm, l_{3_H}'' = 12.1 mm, w_3'' = 0.1 mm.

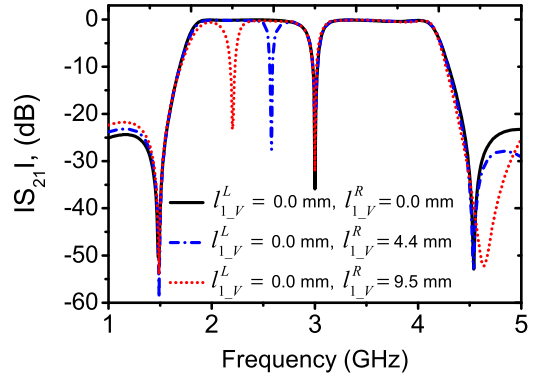

(a)

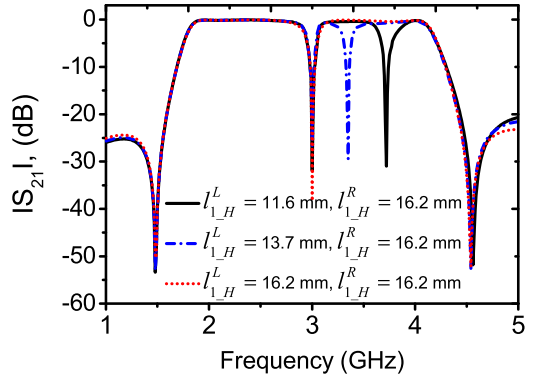

(b)

FIGURE 12. The filter responses respect to different (a) $l_{1\_V}^R$ ($l_{1\_H}^L = l_{1\_H}^R$ = 16.2 mm); (b) $l_{1\_H}^L$ ($l_{1\_V}^L = l_{1\_V}^L$ = 0 mm). The other parameters are: l_F = 16.2 mm, w_F = 0.3 mm, s_F = 0.1 mm, w_1 = 0.3 mm, s_1 = 0.3 mm, l_2 = 15.7 mm, w_2 = 1.4 mm, l_3' = 16.6 mm, w_3' = 0.1 mm, l_{3_V}'' = 4.6 mm, l_{3_H}'' = 12.1 mm, w_3'' = 0.1 mm.

D. SIMULATED AND MEASURED RESULTS

For the designed NWB BPF with a notch band at 3.0 GHz, its measured results are compared with the simulated ones in Fig. 13 (a). Apparently, the measured frequency responses agree well with the simulated ones. The measured pass-band range is from 1.74 to 4.19 GHz with center frequency

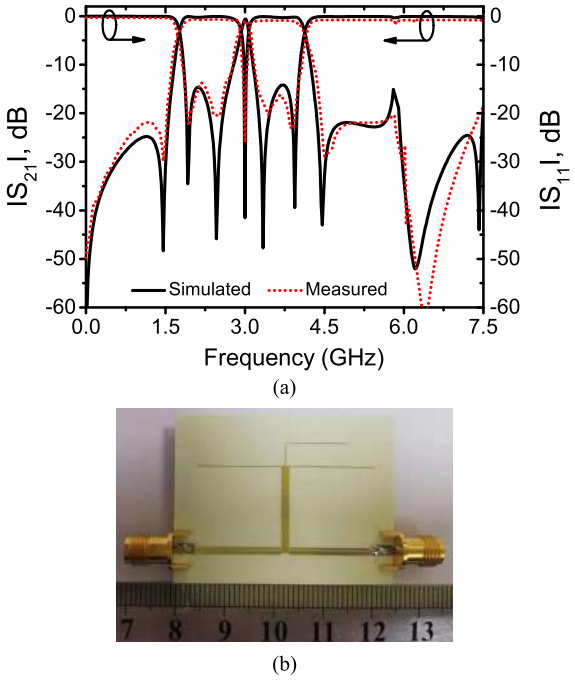

FIGURE 13. (a) The simulated and measured results of Filter I; (b) The photograph of Filter I.

of 2.97 GHz when the impedance matching is better than 10.0 dB, and the minimum insertion loss is 0.55 dB in the passband. Therefore, the corresponding FBW is 82.6%. Four TPs are observed at 1.86, 2.46, 3.38, and 3.98 GHz respectively, ensuring the wide passband and excellent flatness. Two TZs for wide stopbands are located at 0 and 6.38 GHz. Over 20-dB attenuation in the lower and upper stopbands is realized from DC to 1.51 GHz and 4.45 to 7.50 GHz, indicating a high isolation level. The attenuation slop in the lower and upper transition bands is 217 and 64 dB/GHz, with two TZs for sharp selectivity located at 1.44 and 4.64 GHz. A notch band with isolation loss more than 25 dB is found at 3.01 GHz. The in-band variation of the measured group delay is smaller than 0.27 ns, showing a good passband linearity. In Fig. 13 (b), the photograph is illustrated.

III. RECONFIGURABLE-BANDWIDTH NWB BPFs

To effectively protect the telecommunication systems from in-band interfering, the bandwidth and center frequencies of the controllable notch bands should be kept fixed when the reconfigurable-bandwidth WB BPFs work in different states. From Section II, it is apparent that the filter bandwidth can be independently controlled by the parameters of TCSR, while the center frequencies and bandwidths of the notch bands are independently controlled by the parameters of the rest parts. Thus, the desired reconfigurable-bandwidth NWB BPFs with controllable notch bands, whose center frequencies and bandwidths can be maintained fixed under different work states, can be designed by inserting some tuning elements into the TCSR. To simplify the analysis, only the condition that $\theta_1 = \theta_2 = \theta$ is considered in this paper. One thing should be noted: when $\theta_1 \neq \theta_2$, the proposed reconfigurable BPFs will own two controllable notch bands, whose center frequencies and bandwidth also can be maintained unaltered under different work states.

A. FILTER II

From Fig. 4(c), it is obvious that Z_3 controls the filter bandwidth, and no effect on the center frequency and notch band. Considering that all the TPs and TZs are symmetrical to f_0, a reconfigurable-bandwidth BPF with fixed notch band and center frequency in each work state can be designed by altering the value of Z_3. To realize this goal, two PIN diodes are inserted, as shown in Fig. 14. By controlling the work states of PIN diodes, the value of Z_3 will be changed. For arbitrary Z_3' and Z_3'', the value of Z_3 can be concluded in Table 1, and the relationship is held as

$$Z_3'' > \frac{Z_3' Z_3''}{Z_3' + Z_3''} > \frac{2Z_3' Z_3''}{2Z_3' + Z_3''}. \tag{13}$$

As such, the filter bandwidth will be increased when the work states of PIN diodes are altered from Case A to C.

To validate this, a reconfigurable NWB BPF with three bandwidth states is designed on a substrate called Rogers RO4003C with dielectric constant of 3.38 and thickness of 0.813 mm. The circuit parameters should be determined on the basis of the following design procedure at first:

1) Find out the specifications of Filter II with the widest bandwidth, including center frequency, filter bandwidth, selectivity, and notch bandwidth.
2) According to the design procedure of Filter I, determine the parameters of Z_1, Z_2, Z_3'', Z_{oe}, Z_{oo}.

TABLE 1. The Value of Z_3 with different status of PIN diodes.

	Case A	Case B	Case C
D_1	Off	On (Off)	On
D_2	Off	Off (On)	On
Z_3	Z_3''	$\frac{Z_3' Z_3''}{Z_3' + Z_3''}$	$\frac{2Z_3' Z_3''}{2Z_3' + Z_3''}$

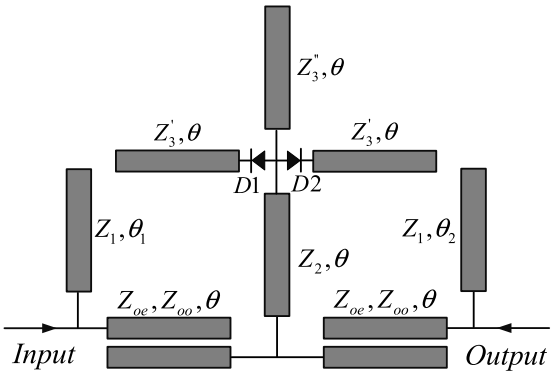

FIGURE 14. The topology of the reconfigurable-bandwidth NWB BPFs with fixed center frequency (Filter II).

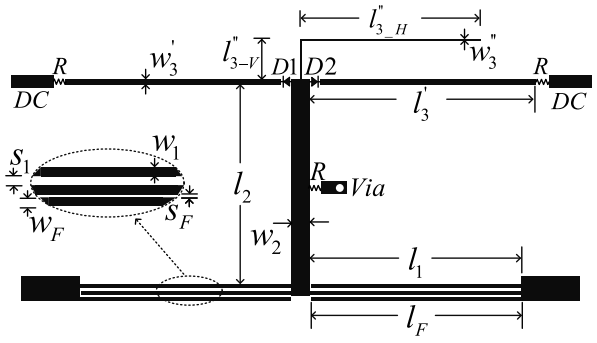

FIGURE 15. The layout of Filter II.

3) Based on the specifications of Filter II with the rest two filter bandwidths, determine the parameter of Z_3'.
4) Slightly adjust the parameters of Z_1, Z_2, Z_3', Z_3'', Z_{oe} and Z_{oo} to obtain the desired performances.

Based on the design procedure mentioned above, the circuit parameters can be generalized as: $Z_1 = 1700\ \Omega$, $Z_2 = 65\ \Omega$, $Z_3' = 143.1\ \Omega$, $Z_3'' = 220\ \Omega$, $Z_{oe} = 162\ \Omega$, $Z_{oo} = 58\ \Omega$, and $\theta_1 = \theta_2 = \theta = 90°$. As such, the value of Z_3 is 220, 87.6, and 54 Ω for Case A to C, respectively. The filter layout is shown in Fig. 15. Two PIN diodes called MADP-000907-14020 are used as the tuning elements, whose dimensions are 0.2 mm×0.2 mm×0.5 mm. They can be modelled by a lumped-element capacitor of 0.025 pF for isolation and 5.2 Ω for connection. In addition, two DC sources are used to control the work states of the inserted PIN diodes, three lumped resistors with large value are used as the protective element and radio frequency (RF) choke. For the final dimensions, they are summarized as (unit: mm): $l_F = 16.2$, $w_F = 0.3$, $s_F = 0.1$, $l_1 = 16.3$, $w_1 = 0.3$, $s_1 = 0.3$, $l_2 = 15.3$, $w_2 = 1.4$, $l_3' = 16.8$, $w_3' = 0.4$, $l_{3\_}''V = 3.1$, $l_{3\_}''H = 13.85$, $w_3'' = 0.1$. The overall circuit size is 43.0 mm× 33.0 mm (0.62 $\lambda_g \times$ 0.48 λ_g, where λ_g is the guided wavelength in the used substrate at center frequency).

For the simulated and measured results of Case A (minimum bandwidth), Case B (medium bandwidth), and Case C (maximum bandwidth), they are illustrated in Fig. 16 and summarized in Table 2. Apparently, the measured results agree well with the simulated ones. With the help of the suitable DC bias and tuning elements, the absolute bandwidth (ABW) can be reconfigurable from 1.22 to 2.46 GHz, while the center frequency and notch band are maintained about 2.94 and 3.01 GHz, respectively. Hence, the FBW is varied from 41.6% to 83.4% with 41.8% tuning range. In the passband, the measured average insertion loss is about 1.9 dB, and the measured return loss is better than 10.0 dB. The in-band variation of measured group delay is smaller than 0.87 ns. Besides, 20-dB insertion loss is observed in notch band. In Fig. 17, the photograph of Filter II is shown.

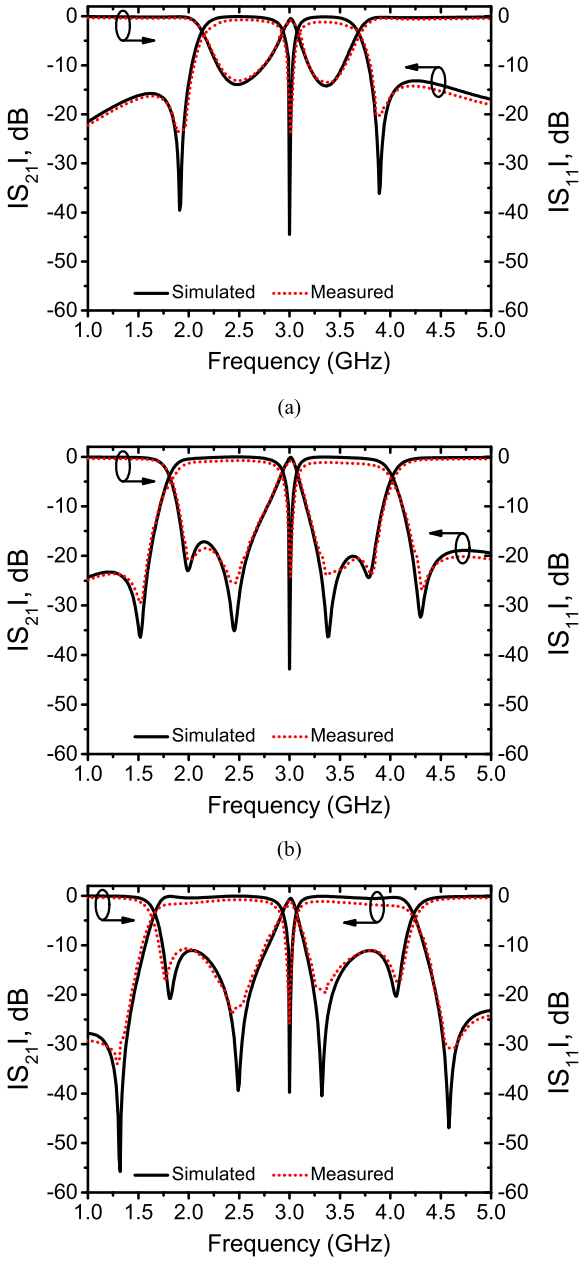

FIGURE 16. Simulated and measured *S*-parameters of Filter II under (a) Case A (minimum bandwidth); (b) Case B (medium bandwidth); (c) Case C (maximum bandwidth).

TABLE 2. Simulated and measured results.

		CF (GHz)	Notch band (GHz)	ABW (GHz)	FBW (%)
Case A (Minimum BW)	Simulated	2.91	3.0	2.29 – 3.53	42.6%
	Measured	**2.93**	**3.01**	**2.32 - 3.54**	**41.6%**
Case B (Medium BW)	Simulated	2.91	3.0	1.89 – 3.93	70.1%
	Measured	**2.93**	**3.02**	**1.91 – 3.94**	**69.4%**
Case C (Maximum BW)	Simulated	2.95	3.0	1.74 – 4.15	81.8%
	Measured	**2.94**	**3.00**	**1.71 – 4.17**	**83.4%**

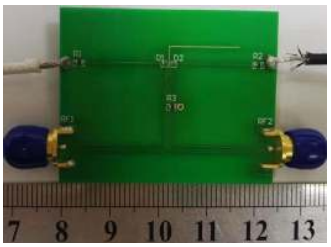

FIGURE 17. The photograph of Filter II.

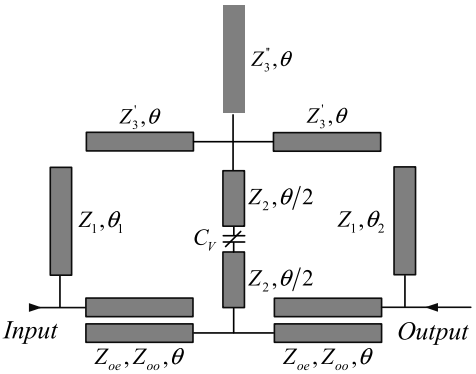

FIGURE 18. Topology of the reconfigurable-bandwidth NWB BPFs with fixed upper passband edge (Filter III).

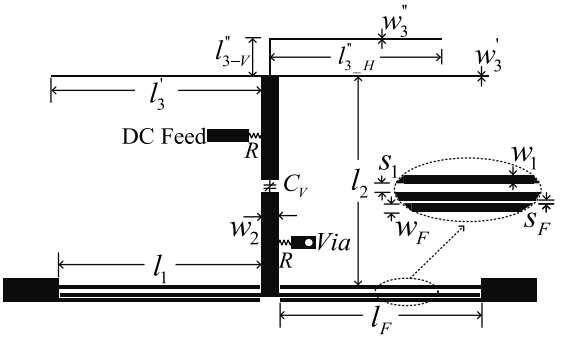

FIGURE 19. The layout of Filter III.

B. FILTER III

The equivalent circuit of Filter III is plotted in Fig. 18. The independently tunable lower passband edge is achieved by inserting a varactor into lower stub of TCSR. By varying the supplied voltage of DC source, the capacitance C_V will be altered. For a NWB BPF based on the proposed topology, C_V has much greater effect on the lower passband edge than the upper one while no effect on the notch band. Hence, the desired reconfigurable-bandwidth NWB BPFs with fixed upper passband edge and notch band in each work state can be achieved by using the proposed topology.

To verify this, a NWB BPF based on the proposed topology is implemented on a substrate called Rogers RO4003C. At first, the circuit parameters should be determined based on the following design procedure:

1) Input the specifications of Filter III with the widest bandwidth, including center frequency, selectivity, filter bandwidth, and notch bandwidth.

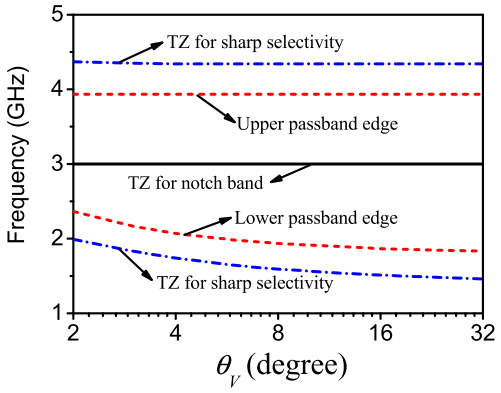

FIGURE 20. Filter responses respect to different C_V.

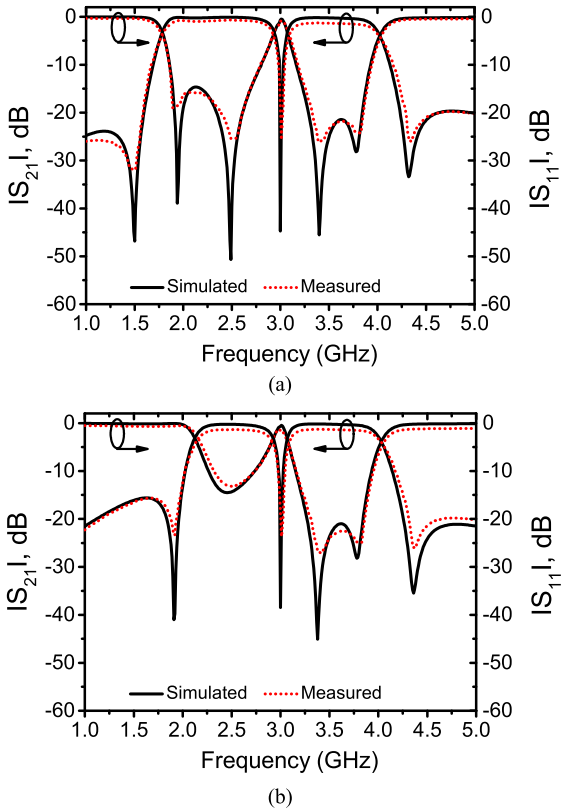

FIGURE 21. The simulated and measured S-parameters of Filter III when the supplied voltage of DC source is (a) 0 V, and (b) 20 V.

2) Based on the design procedure of Filter I, determine the parameters of Z_1, Z_2, Z_3', Z_3'', Z_{oe}, Z_{oo}.
3) According to the requirements of Filter III with narrowest bandwidth, determine the value of C_V.
4) Slightly adjust the parameters of Z_1, Z_2, Z_3', Z_3'', Z_{oe}, Z_{oo}, and C_V to obtain the desired performances.

According to the design procedure mentioned above, the final circuit of Filter III can be summarized as: $Z_1 = 1700\ \Omega$, $Z_2 = 65\ \Omega$, $Z_3 = 84\ \Omega$, $Z_{oe} = 162\ \Omega$, $Z_{oo} = 58\ \Omega$, $\theta = 90°$, $C_V = 18.22$ pF (wide bandwidth), and $C_V = 2.38$ pF (narrow bandwidth). With the help of commercial software, the lay-out can be determined, as plotted in Fig. 19.

TABLE 3. Comparison with previous works.

	CFs (GHz)	TPs/ TZs	RB[1]	Number of tuning elements	Number of tuning states	Number of notch bands	CNB[2]	FBNB[3]	Group delay (ns)	FBW tuning rang (%)	Circuit size ($\lambda g \times \lambda g$)
[15]	3.03	3/3	No	0	0	2	No	No	< 1.0	107	0.89 × 0.46
[21]	4.55	6/3	No	0	0	1	No	No	< 0.75	94.1	0.86 × 0.49
Filter C in [22]	6.80	4/4	No	0	0	1	No	No	< 0.7	82.4	0.47 × 0.22
[24]	3.36	4/3	No	1	Multiple	2	No	No	N/A	75.6	0.49 × 0.49
Filter II in [29]	2.01	7/6	Yes	4	3	2	No	No	< 3.8	74.8-92.1 (17.3)	0.76 × 0.76
Filter III in [29]	2.02	7/6	Yes	1	Multiple	2	No	No	< 4.2	85.3 -94.2 (8.9)	0.76 × 0.76
Filter I	**2.97**	**4/5**	**Yes**	**0**	**0**	**1**	**Yes**	**No**	**< 0.47**	**82.6**	**0.62 × 0.48**
Filter II	**2.94**	**4/5**	**Yes**	**2**	**3**	**1**	**Yes**	**Yes**	**< 3.9**	**41.6–83.4 (41.8)**	**0.62 × 0.48**
Filter III	**2.95**	**4/5**	**Yes**	**1**	**Multiple**	**1**	**Yes**	**Yes**	**< 4.3**	**54.9-70.9 (15.6)**	**0.62 × 0.48**

RB[1]: reconfigurable-bandwidth; CNB[2]: both bandwidth and locations of notch bands can be controlled; FBNB[3]: the notch bandwidth will be kept unchanged under different bandwidth states.

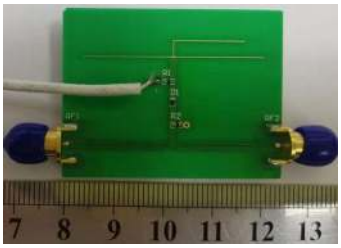

FIGURE 22. The photograph of Filter III.

In this design, a varactor called SMV1235 is used as the tuning elements, whose typical capacitance is varied from 2.38 to 18.22 pF, while series resistance and inductance are 0.60 Ω and 0.45 nH respectively. Besides, the varactor dimension is 0.5 mm×0.6 mm×1.0 mm. Two lumped resistors with large value are used as the protective elements and RF choke. For the final dimensions, they can be generalized as follows (unit: mm): $l_F = 16.2$, $w_F = 0.3$, $s_F = 0.1$, $l_1 = 16.3$, $w_1 = 0.3$, $s_1 = 0.3$, $l_2 = 16.6$, $w_2 = 1.4$, $l'_3 = 16.9$, $w'_3 = 0.1$, $l''_{3\_V} = 3.1$, $l''_{3\_H} = 13.9$, $w''_3 = 0.1$. The overall circuit size is 43.0 mm× 33.0 mm (0.62 λ_g× 0.48 λ_g, where the λ_g is the guided wavelength in the used substrate at center frequency).

In Fig. 20, the relationships among C_V, TZs for notch band and sharp selectivity, and upper/lower passband edges are plotted. It is apparent that the lower passband edge will move upwards with the decrease of C_V, while the upper one and notch band with TZ for sharp selectivity near the upper passband edge are kept unaltered. Besides, the TZ for sharp selectivity near lower passband edge also moves upwards with the decrease of C_V. This phenomenon can ensure the good selectivity for each work states near the lower pass-band edge. Therefore, the desired reconfigurable-bandwidth NWB BPFs can be designed by using this design topology.

In Fig. 21, the measured S-parameters are compared with the simulated ones. When the supplied voltage is 0 V, the proposed filter owns a maximum bandwidth of 2.08 GHz from 1.86 to 3.94 GHz. When supplied voltage is 20 V, the proposed filter owns a minimum bandwidth of 1.62 GHz from 2.33 to 3.95 GHz. If the center frequency is assumed as 2.95 GHz, the FBW can be varied from 54.9% to 70.5%. Therefore, the FBW tuning range is 15.6%. Besides, the measured insertion loss is better than 1.6 dB, and the return loss is better than 10 dB. The in-band variation of measured group delay is smaller than 0.91 ns. Furthermore, a notch band with 20-dB insertion loss is found at about 3.02 GHz. Besides, the TZ for sharp selectivity near the lower pass-band edge is elevated from 1.44 to 1.91 GHz when the DC voltage changes from 0 to 20 V. In Fig. 22, the photograph of Filter III is shown.

To highlight the advantages of the proposed NWB BPFs, the comparisons with some previous works are listed in Table 3. As the third reported works about reconfigurable-bandwidth NWB BPFs, the center frequency and bandwidth of the notch band not only can be independently controlled, but also kept unaltered under different work states. Besides, they also own wider tuning ranges. Hence, they not only can be used to reduce the design complexity and system size, but also prevent the high data-rata telecommunication transceivers from in-band interference more effectively and conveniently. Furthermore, NWB BPFs with independently reconfigurable notch bands and bandwidth can be designed by inserting some varactors into the open-ended stubs of the topologies for the design of Filter II and III.

IV. CONCLUSION

A series of novel topologies for the design of reconfigurable-bandwidth NWB BPFs with controllable notch bands, whose center frequencies and bandwidths are fixed under different

work states, are proposed in this paper. Theoretical analysis finds that the center frequencies and bandwidth of the notch bands not only can be independently controlled, but also kept unaltered under different bandwidth states. Three prototypes are designed and fabricated. All the filters have successfully demonstrated wide bandwidth and tuning ranges, excellent passband flatness, high isolation level, and sharp selectivity. It is anticipated that this simple methodology can be broadly used in multi-standard microwave communication systems

REFERENCES

[1] F.-C. Chen, R.-S. Li, and Q. X. Chu, "Ultra-wide stopband low-pass filter using multiple transmission zeros," *IEEE Access*, to be published.
[2] Y. Wu, L. Cui, W. Zhang, L. Jiao, Z. Zhuang, and Y. Liu, "High performance single-ended wideband and balanced bandpass filters loaded with stepped-impedance stubs," *IEEE Access*, vol. 5, pp. 5972–5981, 2017.
[3] X. Jin, X. Huang, D. Chen, and C. Cheng, "Response diversity of stub-loaded ring bandpass filter based on commensurate line element: Single- and dual-band applications," *IEEE Access*, vol. 7, pp. 25681–25689, 2019.
[4] D. Psychogiou, R. Gomez-Garcia, and D. Peroulis, "RF wide-band bandpass filter with dynamic in-band multi-interference suppression capability," *IEEE Trans. Circuits Syst., II, Exp. Briefs*, vol. 65, no. 7, pp. 898–902, Jul. 2018.
[5] J.-K. Xiao, X. Qi, H.-X. Wang, and J.-G. Ma, "High selective balanced bandpass filters using end-connected conductor-backed coplanar waveguide," *IEEE Access*, vol. 7, pp. 16184–16193, 2019.
[6] W. Feng, X. Gao, W. Che, W. Yang, and Q. Xue, "High selectivity wideband balanced filters with multiple transmission zeros," *IEEE Trans. Circuits Syst., II, Exp. Briefs*, vol. 64, no. 10, pp. 1182–1186, Oct. 2017.
[7] W.-J. Zhou and J.-X. Chen, "High-selectivity tunable balanced bandpass filter with constant absolute bandwidth," *IEEE Trans. Circuits Syst., II, Exp. Briefs*, vol. 64, no. 8, pp. 917–921, Aug. 2017.
[8] Y. Xie, F.-C. Chen, and Z. Li, "Design of dual-band bandpass filter with high isolation and wide stopband," *IEEE Access*, vol. 5, pp. 25602–25608, 2017.
[9] A. Saghir, A. Quddious, S. Arain, P. Vryonides, and S. Nikolaou, "Single-/Dual-BPF using coupled-line stepped impedance resonators (CLSIR)," *IEEE Trans. Circuits Syst., II, Exp. Briefs*, vol. 66, no. 9, pp. 1497–1501, Sep. 2019.
[10] X.-K. Bi, X. Zhang, S.-W. Wong, T. Yuan, and S.-H. Guo, "Design of equal-ripple dual-wideband bandpass filter with minimum design parameters based on cross-shaped resonator," *IEEE Trans. Circuits Syst., II, Exp. Briefs*, to be published, doi: 10.1109/TCSII.2019.2951781.
[11] X.-K. Bi, T. Cheng, P. Cheong, S.-K. Ho, and K.-W. Tam, "Design of dual-band bandpass filters with fixed and reconfigurable bandwidths based on terminated cross-shaped resonators," *IEEE Trans. Circuits Syst., II, Exp. Briefs*, vol. 66, no. 3, pp. 317–321, Mar. 2019.
[12] J. Ni and J. Hong, "Compact varactor-tuned microstrip high-pass filter with a quasi-elliptic function response," *IEEE Trans. Microw. Theory Techn.*, vol. 61, no. 11, pp. 3853–3859, Nov. 2013.
[13] C. Cui and Y. Liu, "Quad-band bandpass filter design by embedding dual-band bandpass filter with dual-mode notch elements," *Electron. Lett.*, vol. 50, no. 23, pp. 1719–1720, Nov. 2014.
[14] Y. Song, G.-M. Yang, and W. Geyi, "Compact UWB bandpass filter with dual notched bands using defected ground structures," *IEEE Microw. Wireless Compon. Lett.*, vol. 24, no. 4, pp. 230–232, Apr. 2014.
[15] L. Yang, W.-W. Choi, K.-W. Tam, and L. Zhu, "Novel wideband bandpass filter with dual notched bands using stub-loaded resonators," *IEEE Microw. Wireless Compon. Lett.*, vol. 27, no. 1, pp. 25–27, Jan. 2017.
[16] K. Song and Q. Xue, "Compact ultra-wideband (UWB) bandpass filters with multiple notched bands," *IEEE Microw. Wireless Compon. Lett.*, vol. 20, no. 8, pp. 447–449, Aug. 2010.
[17] C. Ho Kim and K. Chang, "Ultra-wideband (UWB) ring resonator bandpass filter with a notched band," *IEEE Microw. Wireless Compon. Lett.*, vol. 21, no. 4, pp. 206–208, Apr. 2011.
[18] G.-M. Yang, R. Jin, C. Vittoria, V. G. Harris, and N. X. Sun, "Small ultra-wideband (UWB) bandpass filter with notched band," *IEEE Microw. Wireless Compon. Lett.*, vol. 18, no. 3, pp. 176–178, Mar. 2008.
[19] B. Mohammadi, P. Rezaei, J. Nourinia, and A. Valizade, "Design of a compact dual-band-notch ultra-wideband bandpass filter based on wave cancellation method," *IET Microw., Antennas Propag.*, vol. 9, no. 1, pp. 1–9, Jan. 2015.
[20] X. Chen, L. Zhang, and Y. Peng, "UWB bandpass filter with sharp rejection and narrow notched band," *Electron. Lett.*, vol. 50, no. 15, pp. 1077–1079, Jul. 2014.
[21] X.-K. Bi, X. Zhang, G.-L. Huang, and T. Yuan, "Compact microstrip NWB/DWB BPFs with controllable isolation bandwidth for interference rejection," *IEEE Access*, vol. 7, pp. 49169–49176, 2019.
[22] H. Wang, K.-W. Tam, S.-K. Ho, W. Kang, and W. Wu, "Design of ultra-wideband bandpass filters with fixed and reconfigurable notch bands using terminated cross-shaped resonators," *IEEE Trans. Microw. Theory Techn.*, vol. 62, no. 2, pp. 252–265, Feb. 2014.
[23] L. Kurra, M. P. Abegaonkar, A. Basu, and S. K. Koul, "Switchable and tunable notch in ultra-wideband filter using electromagnetic bandgap structure," *IEEE Microw. Wireless Compon. Lett.*, vol. 24, no. 12, pp. 839–841, Dec. 2014.
[24] D. Psychogiou, R. Gomez-Garcia, and D. Peroulis, "Fully adaptive multi-band bandstop filtering sections and their application to multifunctional components," *IEEE Trans. Microw. Theory Techn.*, vol. 64, no. 12, pp. 4405–4418, Dec. 2016.
[25] D. Psychogiou, R. Gomez-Garcia, and D. Peroulis, "Wide-passband filters with in-band tunable notches for agile multi-interference suppression in broad-band antenna systems," in *Proc. IEEE Radio Wireless Symp. (RWS)*, Anaheim, CA, USA, Jan. 2018, pp. 213–216.
[26] W. Feng, Y. Shang, and W. Che, "Ultra-wideband bandpass filter with reconfigurable notch bands using TCSRs," *Electron. Lett.*, vol. 51, no. 23, pp. 1893–1894, Nov. 2015.
[27] R. Zhang, R. Gomez-Garcia, and D. Peroulis, "Multifunctional bandpass filters with reconfigurable and switchable band control," *IEEE Trans. Microw. Theory Techn.*, vol. 67, no. 6, pp. 2355–2369, Jun. 2019.
[28] C. Teng, P. Cheong, and K.-W. Tam, "Reconfigurable wideband bandpass filters based on dual cross-shaped resonator," in *IEEE MTT-S Int. Microw. Symp. Dig.*, May 2019, pp. 1–3.
[29] X.-K. Bi, C. Teng, P. Cheong, S.-K. Ho, and K.-W. Tam, "Wideband bandpass filters with reconfigurable bandwidth and fixed notch bands based on terminated cross-shaped resonator," *IET Microw., Antennas Propag.*, vol. 13, no. 6, pp. 796–803, 2019.
[30] R. Li, S. Sun, and L. Zhu, *Microwave Bandpass Filters for Wideband Communications*. Hoboken, NJ, USA: Wiley, 2012, pp. 18–84.

XIAO-KUN BI was born in Henan, China, in 1987. He received the B.Sc. degree in electrical and information engineering from the North University of China, Taiyuan, China, in 2010, the M.Sc. degree in signal and information processing from Nankai University, Tianjin, China, in 2015, and the Ph.D. degree in electrical and computer engineering from the University of Macao, Taipa, Macao, in 2019.

In 2014, he was a Research Assistant with the University of Macao, Taipa, Macao. His research interests include notched-/dual-wideband bandpass filters, reconfigurable filters, slotline antennas, and their applications in modern communication systems.

XIAO ZHANG (Member, IEEE) was born in Gaozhou, China. He received the B.Eng. degree in information engineering and the M.Eng. degree in communication and information systems from the South China University of Technology, Guangzhou, China, in 2011 and 2014, respectively, and the Ph.D. degree in electrical and computer engineering from the University of Macau, Macau, China, in 2017.

From September 2012 to August 2014, he was a Research Assistant with Comba Telecom Systems Limited, Guangzhou. He joined the Antenna and Electromagnetic-Wave Laboratory, University of Macau, as a Research Fellow, in January 2018. He is currently an Assistant Professor with the College of Information Engineering, Shenzhen University, Shenzhen, China. His research interests include planar antennas and microwave circuits.

SAI-WAI WONG (Senior Member, IEEE) received the B.S. degree in electronic engineering from The Hong Kong University of Science and Technology, Hong Kong, in 2003, and the M.Sc. and Ph.D. degrees in communication engineering from Nanyang Technological University, Singapore, in 2006 and 2009, respectively.

From July 2003 to July 2005, he was the Lead Engineering Department in mainland of China with two Hong Kong manufacturing companies. From 2009 to 2010, he was a Research Fellow with the Institute for Infocomm Research, Singapore. Since 2010, he has been an Associate Professor and became a Full Professor with the School of Electronic and Information Engineering, South China University of Technology, Guangzhou, China. In 2016, he was a Visiting Professor with the City University of Hong Kong. In 2017, he was a Visiting Professor with the University of Macau. Since 2017, he has been a Full Professor with the College of Electronic and Information Engineering, Shenzhen University, Shenzhen, China. His current research interests include RF/microwave circuit and antenna design.

Dr. Wong was a recipient of the New Century Excellent Talents in University (NCET) Award, in 2013, and the Shenzhen Overseas High-Caliber Personnel Level C, in 2018. He is currently a Reviewer for several top-tier journals.

SHAO-HUA GUO was born in Henan, China, in 1994. She received the B.Sc. degree from the North China University of Water Resources and Electric Power, Zhengzhou, China, in 2018. She is currently pursuing the M.Sc. degree with Zhengzhou University, Zhengzhou.

TAO YUAN (Member, IEEE) received the bachelor's and master's degrees from Xidian University, China, and the Ph.D. degree from the National University of Singapore, Singapore. He is currently a Professor with the College of Information Engineering, Shenzhen University, Shenzhen, China. His current research interests include developing novel RF modules and antennas for mobile terminal and 5G applications.